

¹ Derotation: a Python package for correcting rotation-induced distortions in line-scanning microscopy

⁴ **Laura Porta**  ¹, **Simon Weiler**  ¹, **Adam L. Tyson**  ², and **Troy W. Margrie**  ¹

⁶ 1 The Sainsbury Wellcome Centre for Neural Circuits and Behaviour, University College London, 25
⁷ Howland Street, London W1T 4JG, UK 2 Neuroinformatics Unit, Sainsbury Wellcome Centre & Gatsby
⁸ Computational Neuroscience Unit, University College London, London W1T 4JG, UK

DOI: [10.xxxxxx/draft](https://doi.org/10.xxxxxx/draft)

Software

- [Review](#) 
- [Repository](#) 
- [Archive](#) 

Editor: 

Submitted: 22 October 2025

Published: unpublished

License

Authors of papers retain copyright and release the work under a Creative Commons Attribution 4.0 International License ([CC BY 4.0](https://creativecommons.org/licenses/by/4.0/))

⁹ Summary

¹⁰ Line-scanning microscopy, including multiphoton calcium imaging of neural populations *in vivo*,
¹¹ is a powerful technique for observing dynamic processes at cellular resolution. However, when
¹² the imaged sample rotates during acquisition (for example during horizontal passive rotation),
¹³ the sequential line-by-line scanning process introduces geometric distortions. These artifacts,
¹⁴ which manifest as shearing or curving of features, can severely compromise downstream analyses
¹⁵ such as motion registration, cell detection, and signal extraction. While several studies have
¹⁶ developed custom solutions for this issue (Vélez-Fort et al., 2018), (Hennestad et al., 2021),
¹⁷ (Sit & Goad, 2023), (Voigts & Harnett, 2020), a general-purpose, accessible software package
¹⁸ has been lacking.

¹⁹ derotation is an open-source Python package that algorithmically reconstructs image frames
²⁰ from data acquired during sample rotation around an axis orthogonal to the imaging plane. By
²¹ leveraging recorded rotation angles and the microscope's line acquisition clock, the software
²² applies a precise, line-by-line inverse transformation to restore the expected geometry of
²³ the imaged plane. This correction enables reliable cell segmentation during rapid rotational
²⁴ movements, making it possible to study yaw motion without sacrificing image quality (Figure
²⁵ 1).

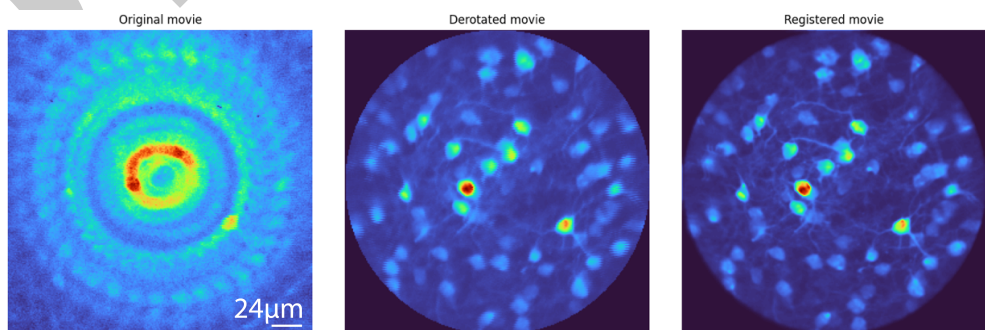


Figure 1: Example of derotation correction. On the left, the average of a series of images acquired using 3-photon microscopy of layer 6 mouse cortical neurons labeled with GCaMP7f during passive rotation. Center, the mean image after derotation, and on the left the mean image of the derotated movie after suite2p registration (Pachitariu et al., 2016). As you can see, following derotation the cells are visible and have well defined shapes.

²⁶ Statement of Need

²⁷ Any imaging modality that acquires data sequentially, such as line-scanning microscopy, is
²⁸ susceptible to motion artifacts if the sample moves during the acquisition of a single frame.
²⁹ When this motion is rotational, it produces characteristic “fan-like” distortions that corrupt the
³⁰ morphological features of the imaged structures (Figure 2). This significantly complicates, or
³¹ even prevents, critical downstream processing steps such as cell segmentation and automated
³² region-of-interest tracking.

³³ This problem is particularly acute in systems neuroscience, where researchers increasingly
³⁴ combine two-photon or three-photon calcium imaging with behavioral paradigms involving
³⁵ head rotation (Vélez-Fort et al., 2018), (Hennestad et al., 2021), (Sit & Goad, 2023), (Voigts
³⁶ & Harnett, 2020). In such experiments, where head-fixed animals may be passively or actively
³⁷ rotated, high-speed angular motion can render imaging data unusable. The issue is even
³⁸ more problematic for imaging modalities with lower frame rates, such as three-photon calcium
³⁹ imaging. While individual labs have implemented custom scripts to address this, there remains
⁴⁰ no validated, open-source, and easy-to-use Python tool available to the broader community.

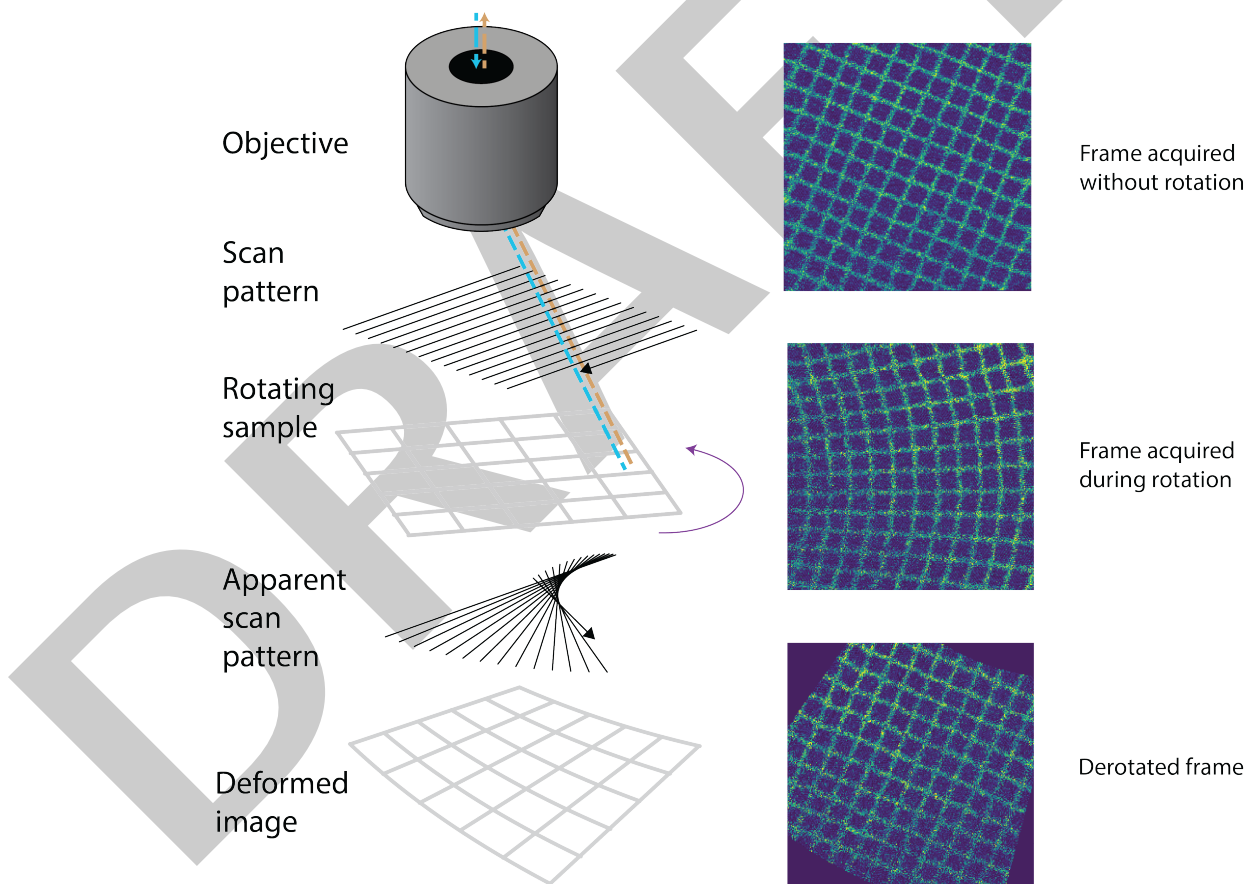


Figure 2: Schematic of line-scanning microscope distortion. Left: line scanning pattern plus sample rotation lead to fan-like artifacts when imaging a grid. Right: grid imaged while still (top), while rotating at 200°/s with 7Hz frame rate (middle), and after derotation (bottom), showing alignment restoration.

⁴¹ derotation meets this need by providing a documented, tested, and modular solution for post
⁴² hoc correction of imaging data acquired during rotation. It enables researchers to perform
⁴³ quantitative imaging during high-speed rotational movements. By providing a robust and
⁴⁴ accessible tool, derotation lowers the barrier for entry into complex behavioral experiments
⁴⁵ and improves the reproducibility of a key analysis step in a growing field of research.

46 **Functionality**

47 The core of the derotation package is a line-by-line affine transformation. It operates by first
48 establishing a precise mapping between each scanned line in the movie and the rotation angle
49 of the sample at that exact moment in time. It then applies an inverse rotation transform
50 to each line around a specified or estimated center of rotation. Finally, the corrected lines
51 are reassembled into frames, producing a movie that appears as if the sample had remained
52 stationary.

53 **Modular Design**

54 derotation is designed with modularity in mind, catering to both novice users and advanced
55 programmers.

56 **End to end Pipelines**

57 For ease of use, derotation provides two high-level processing workflows tailored to common
58 experimental paradigms. The pipelines are designed for experimental setups with synchronized
59 rotation and imaging data. The required inputs are:

- 60 ▪ Arrays of analog signals containing timing and rotation information, typically including
61 the start of a new line, the start of a new frame, when the rotation system is active, the
62 rotation position feedback;
- 63 ▪ A CSV file describing speeds and directions.
- 64 ▪ FullPipeline is engineered for experimental paradigms involving randomized, clockwise
65 or counter-clockwise rotations. It assumes that there will be complete 360° rotations of
66 the sample. As part of its workflow, it can optionally estimate the center of rotation
67 automatically using Bayesian optimization, which minimizes residual motion in the
68 corrected movie.
- 69 ▪ IncrementalPipeline is optimized for stepwise, single-direction rotations. This rotation
70 paradigm is useful for calibration of the luminance across rotation angles. It can also
71 provide an alternative estimate of the center of rotation, fitting the trajectory of a cell
72 across rotation angles.

73 Both pipelines are configurable via YAML files or Python dictionaries, promoting reproducible
74 analysis by making it straightforward to document and re-apply the same parameters across
75 multiple datasets.

76 Upon completion, a pipeline run generates a comprehensive set of outputs: the corrected
77 movie, a CSV file with rotation angles and metadata for each frame, debugging plots, a text
78 file containing the estimated optimal center of rotation, and log files with detailed processing
79 information.

80 **Low-level core function**

81 Advanced users can bypass pipeline workflows and use the core line-by-line derotation function
82 directly by providing the original movie and an array of rotation angles for each line.

83 This modular design allows users with custom experimental setups to integrate the derotation
84 algorithm into their own analysis scripts while still benefiting from the line-by-line derotation
85 logic.

86 Validation

87 Using 3-photon imaging data from head-fixed mice

88 The package's effectiveness has been validated on three-photon recordings of deep cortical
 89 neurons expressing the calcium indicator GCaMP7f in head-fixed mice (Figure 3). The
 90 corrected images showed restored cellular morphology and were successfully processed by
 91 standard downstream signal analysis pipelines such as Suite2p ([Pachitariu et al., 2016](#)). In
 92 Figure 3, it is possible to compare the change in fluorescence ($\Delta F/F_0$) of two regions of
 93 interest (ROIs) in the case of line-by-line derotation (as implemented in derotation) and frame-
 94 by-frame derotation (using `scipy.ndimage.affine_transform`). The line-by-line derotation
 95 restores the $\Delta F/F_0$ to its original value during rotation times, reducing the dips into negative
 96 values that are present in the frame-by-frame derotation.

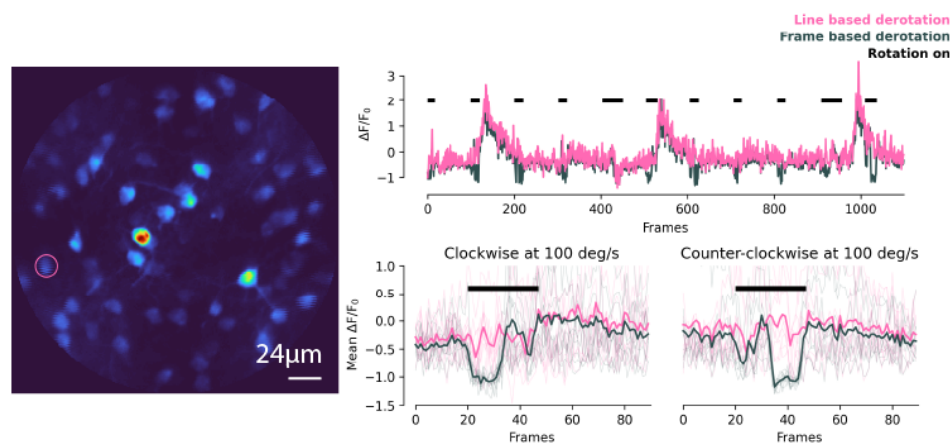


Figure 3: Figure 3. Validation on 3-photon data. Left: mean image after line-by-line derotation. Red circle marks the ROI used for the plots on the right. Top right: sample $\Delta F/F_0$ timecourse for the selected ROI (pink = line-by-line derotation; gray = frame-by-frame affine correction; shaded vertical bars = rotation intervals). Bottom right: mean $\Delta F/F_0$ aligned to rotation periods for clockwise and counterclockwise rotations. Line-by-line derotation preserves the ROI signal during rotations and removes the artificial dips introduced by frame-by-frame correction. Clockwise and counterclockwise traces show a roughly mirror-symmetric, angle-dependent modulation of measured fluorescence with the frame-by-frame correction.

97 Synthetic Data Generation

98 derotation includes a synthetic data generator that can create challenging synthetic datasets
 99 with misaligned centers of rotation and out-of-plane rotations. This feature is particularly useful
 100 for validating the robustness of the derotation algorithm and for developing new features.

101 The synthetic data can be generated using the following classes:

- 102 ■ Rotator class: Core class that applies line-by-line rotation to an image stack, simulating
 103 a rotating microscope.
- 104 ■ SyntheticData class: Creates fake cell images, assigns rotation angles, and generates
 105 synthetic stacks leveraging the Rotator class. It is a complete synthetic dataset generator.

106 Documentation and Installation

107 derotation is available on PyPI and can be installed with `pip install derotation`. It
 108 is distributed under a BSD-3-Clause license. Comprehensive documentation, tutorials,

109 and example datasets are available at <https://derotation.neuroinformatics.dev>. Using
110 Binder, users can run the software in a cloud-based environment with sample data without
111 requiring any local installation. The code to reproduce the figures in this paper are
112 available at <https://github.com/neuroinformatics-unit/derotation/joss-paper>. To download
113 the example data used for the figures and the tutorials, please consult the README at
114 <https://github.com/neuroinformatics-unit/derotation/>.

115 Future Directions

116 Derotation is currently used to process 3-photon movies acquired during head rotation. Future
117 directions include further automated pipelines for specific motorised stages and experimental
118 paradigms.

119 Methodological appendix

120 The package has been directly tested on 3-photon imaging data obtained from cortical layer
121 6 callosal-projecting neurons expressing the calcium indicator GCaMP7f in the mouse visual
122 cortex (see Figure 3). More specifically, wild type C57/B6 mice were injected with retro
123 AAV-hSyn-Cre (1×10^{14} units per ml) in the left and with AAV2/1.syn.FLEX.GCaMP7f (1.8
124 $\times 10^{13}$ units per ml) in the right primary visual cortex. A cranial window was implanted over
125 the right hemisphere, and then a headplate was cemented onto the skull of the animal. After 4
126 weeks of viral expression and recovery, animals were head-fixed on a rotation platform driven by
127 a direct-drive motor (U-651, Physik Instrumente). 360 degree clockwise and counter-clockwise
128 rotations with different peak speed profiles (50, 100, 150, 200 deg/s) were performed while
129 imaging awake neuronal activity using a 25x objective (XLPLN25XWMP2, NA 1.05, 25,
130 Olympus). Imaging was conducted at 7 Hz with 256x256 pixels. All experimental procedures
131 were approved by the Sainsbury Wellcome Centre (SWC) Animal Welfare and Ethical Review
132 Body (AWERB). For detailed description of the 3-photon power source and imaging please see
133 ([Cloves & Margrie, 2024](#)).

134 Acknowledgements

135 We thank Eivind Hennestad for initial project discussion. We thank Mateo Vélez-Fort and
136 Chryssanthi Tsitoura for their assistance in building and testing the three-photon imaging
137 and rotation setup as well as for feedback on the package. We also thank Igor Tatarnikov
138 for contributing to the development of the package and the whole Neuroinformatics Unit.
139 This package was inspired by previous work on derotation as described in ([Voigts & Harnett,](#)
140 [2020](#)). The authors are grateful to the support staff of the Neurobiological Research Facility
141 at SWC. This research was funded by the Sainsbury Wellcome Centre core grant from the
142 Gatsby Charitable Foundation (GAT3361) and Wellcome Trust (219627/Z/19/Z), a Wellcome
143 Trust Investigator Award (214333/Z/18/Z) and Discovery Award (306384/Z/23/Z) to T.W.M.
144 and by SWC core funding to the Neurobiological Research Facility. S.W. was funded by a
145 Feodor-Lynen fellowship from the Alexander von Humboldt Foundation.

146 References

- 147 Cloves, M., & Margrie, T. W. (2024). In vivo dual-plane 3-photon microscopy: Spanning
148 the depth of the mouse neocortex. *Biomedical Optics Express*, 15(12), 7022. <https://doi.org/10.1364/BOE.544383>
- 150 Hennestad, E., Witoelar, A., Chambers, A. R., & Vervaeke, K. (2021). Mapping vestibular and
151 visual contributions to angular head velocity tuning in the cortex. *Cell Reports*, 37(12),
152 110134. <https://doi.org/10.1016/j.celrep.2021.110134>

- 153 Pachitariu, M., Stringer, C., Dipoppa, M., Schröder, S., Rossi, L. F., Dalgleish, H., Carandini,
154 M., & Harris, K. D. (2016). *Suite2p: Beyond 10,000 neurons with standard two-photon*
155 *microscopy*. *Neuroscience*. <https://doi.org/10.1101/061507>
- 156 Sit, K. K., & Goard, M. J. (2023). Coregistration of heading to visual cues in retrosplenial cortex.
157 *Nature Communications*, 14(1), 1992. <https://doi.org/10.1038/s41467-023-37704-5>
- 158 Vélez-Fort, M., Bracey, E. F., Keshavarzi, S., Rousseau, C. V., Cossell, L., Lenzi, S. C.,
159 Strom, M., & Margrie, T. W. (2018). A Circuit for Integration of Head- and Visual-
160 Motion Signals in Layer 6 of Mouse Primary Visual Cortex. *Neuron*, 98(1), 179–191.e6.
161 <https://doi.org/10.1016/j.neuron.2018.02.023>
- 162 Voigts, J., & Harnett, M. T. (2020). Somatic and Dendritic Encoding of Spatial Variables in
163 Retrosplenial Cortex Differs during 2D Navigation. *Neuron*, 105(2), 237–245.e4. <https://doi.org/10.1016/j.neuron.2019.10.016>

DRAFT